Light Scattering Study of Heat-Induced Aggregation and Gelation of Ovalbumin

Mireille Weijers and Ronald W. Visschers

Wageningen Centre for Food Science and NIZO Food Research, PO Box 20, 61710 Ede, The Netherlands

Taco Nicolai*

Polymères, Colloïdes, Interfaces, UMR-CNRS, Université du Maine, 72085 Le Mans Cedex 9, France

Received November 19, 2001; Revised Manuscript Received March 6, 2002

ABSTRACT: The effect of ionic strength on the interaction of ovalbumin, a globular egg white protein, in aqueous solution was investigated using static and dynamic light scattering. Strong repulsive interactions are observed at low ionic strength (3 mM). Aggregation of the proteins was induced by heating at low (3 mM) and high (100 mM) ionic strength as a function of the concentration. The size of the aggregates increases with increasing protein concentration and diverges close to the critical concentration for gelation, which is about 60 g/L at low ionic strength and 12 g/L at high ionic strength. Static and dynamic light scattering showed that at low ionic strength linear chains are formed with little branching until close to the gel point, while at high ionic strength denser branched aggregates are formed with a fractal dimension close to that found for other globular protein aggregates. The observations were confirmed by cryo-transmission electron microscopy. Heated systems at low ionic strength remained transparent and were studied in situ using static and dynamic light scattering. The relaxation of the concentration fluctuations occurs by cooperative diffusion, except when the gel point is approached and a slow secondary relaxation process is observed. The slow mode is attributed to the self-diffusion of the aggregates and restructuring of the system. The terminal relaxation time of the concentration fluctuations diverges in the neighborhood of the gel point because a fraction of the concentration fluctuations is progressively frozen in.

Introduction

In general, when globular proteins like ovalbumin or β-lactoglobulin are heated, the molecule unfolds partially, so that parts of the inner hydrophobic region becomes exposed. This denaturation process is usually followed by aggregation, and eventually a gel can be formed.[1] Partly driven by its relevance to industrial applications, heat-induced aggregation of globular proteins has long been a subject of intensive investigation.

Here we investigate the heat-induced aggregation of ovalbumin. Ovalbumin is the most abundant protein in avian egg whites and constitutes over half of the egg white proteins by weight. Egg white proteins possess multiple functional properties in food such as gelling, foaming, water binding, and emulsifying capacity.[2,3] Some of the functionalities relate to structure changes that occur during heat treatment.

Ovalbumin is readily purified and crystallized in gram quantities.[4] It is a monomeric phosphoglycoprotein with a molecular weight of 45 kg/mol and an isoelectric point of 4.5. The complete amino acid sequence, comprising 385 residues, has been determined by Nisbet et al.[5] Purified ovalbumin contains three phophorylated forms, A_1, A_2, and A_3, which contain two, one, and no phosphate groups per molecule, respectively.[6,7] The properties of ovalbumin solutions or gels formed after heat treatment depend on the pH, ionic strength, and protein concentration, and they can be either transparent, opaque, or turbid.[8]

The structure of ovalbumin aggregates has been investigated in detail at pH 7 at low ionic strength.[9−11] At these conditions heated ovalbumin solutions remain transparent. Transmission electron microscopy (TEM) has shown that linear aggregates are formed. It was concluded from static (SLS) and dynamic (DLS) light scattering and intrinsic viscosity measurements that these linear aggregates can be described in terms of the wormlike chain model.[11] When salt is added to screen electrostatic interactions, dense coagulates are observed with TEM.

The purpose of the present work was to study the effect of electrostatic interactions on the aggregation process of ovalbumin at pH 7 by comparing systems at low ($\mu = 3$ mM) and high ($\mu = 0.1$ M) ionic strength. We investigated the effect of the ionic strength on the interactions in native ovalbumin solutions by measuring the concentration dependence of the osmotic compressibility and the cooperative diffusion coefficient. We determined the structure of ovalbumin aggregates formed after extensive heat treatment using SLS and DLS. The method used to characterize the highly diluted aggregates is the same as used earlier for aggregates of another globular protein, β-lactoglobulin.[12,13] A similar SLS study was reported also for bovine serum albumin.[14] Direct comparison of results obtained on different globular proteins is important because it may eventually lead to a general understanding of heat-induced aggregation of globular proteins. The evolution of the structure and the dynamics of the ovalbumin solutions during the aggregation process was studied in situ using SLS and DLS. Measurements on undiluted heated solutions were done only at low ionic strength, because at $\mu = 0.1$ M heated solutions became turbid.

Experimental Section

Materials. The ovalbumin used for this study was purchased from Sigma and used without further treatment. One

10.1021/ma0120198 CCC: $22.00
Published on Web 05/09/2002

batch (I: 30K7054) was used for most experiments, and another batch (II: 19H7002) was sometimes used as specified. The protein content was determined by the Kjeldahl method,[15] using the Kjeldahl factor of 6.12. The protein concentration was 85% for batch I and 88% for batch II. The water content was determined, using Karl Fischer titration,[16] and was found to be 10% for batch I and 6% for batch II. The ovalbumin was dissolved in Millipore water with 3 mM NaN_3 added to avoid bacterial growth. The pH was set at 7 using a NaOH solution. In some cases 0.1 M NaCl was added to screen electrostatic interactions. The solutions were filtered through 0.25 μm pore size Anatop filters. Protein concentrations were measured using refractive index measurements and UV absorption at 280 nm. Consistent results were obtained using refractive index increment $dn/dC = 0.181$ and extinction coefficient $\epsilon = 0.698$ L g^{-1} cm^{-1}. These values are close to those used in the literature.

Methods. Size exclusion chromatography (SEC) experiments were carried out at room temperature with TSK PW 5000 + PW 6000 column set (30 cm + 60 cm) in series and a differential refractive index detector SHODEX RI 71. The columns were eluted with 0.1 M $NaNO_3$ at a flow rate of 1 mL/min. The injected volume was 300 μL, and the injected concentration was around 1.5 g/L.

Cryo-transmission electron microscopy was done at the Unilever Research Center (Vlaardingen, The Netherlands) using a Philips CM12 transmission electron microscope operating at 80 kV. A drop of the liquid sample was placed on a perforated carbon film, supported by a 200 mesh copper grid, and most of the liquid was removed by blotting with a filter paper. The thin liquid films formed across the holes were subsequently vitrified by plunging the grid into liquid propane at a temperature below −170 °C. The specimens were stored in liquid nitrogen until they were transferred to the cryo-holder. The cryo-holder (Oxford) was cooled by liquid nitrogen to a temperature lower than −170 °C. Images were recorded digitally by a Gatan 791 CCD camera using the Digital Micrograph software package.

Static and dynamic light scattering measurements were made using an ALV-5000 multibit multitau correlator and a Spectra Physics solid-state laser operating with vertically polarized light with wavelength $\lambda = 532$ nm. The range of scattering wave vectors covered was $3.0 \times 10^{-3} < q < 3.5 \times 10^{-2}$ nm^{-1} ($q = 4\pi n_s \sin(\theta/2)/\lambda$, with θ the angle of observation and n_s the refractive index of the solution). The temperature was controlled by a thermostat bath to within ±0.1 °C.

Data Analysis. The relative scattering intensity I_r was determined by subtracting the solvant scattering from the total scattering intensity and dividing by the scattering intensity of toluene. I_r is due to concentration fluctuations and is proportional to the osmotic compressibility $(d\pi/dC)^{-1}$ and the structure factor ($S(q)$):[17,18]

$$I_r = KC\frac{RT}{d\pi/dC}S(q) \tag{1}$$

with R the gas constant and T the absolute temperature. $S(q)$ expresses the scattering wave vector dependence of the scattering intensity and is unity for $q \to 0$. K is a contrast factor:

$$K = \frac{4\pi^2 n_s^2}{\lambda^4 N_a}\left(\frac{\partial n}{\partial C}\right)^2\left(\frac{n_{tol}}{n_s}\right)^2\frac{1}{R_{tol}} \tag{2}$$

where N_a is Avogadro's number, $(\partial n/\partial C)$ is the refractive index increment, and R_{tol} is the Rayleigh ratio of toluene at 20 °C ($R_{tol} = 2.79 \times 10^{-5}$ cm^{-1} at $\lambda = 532$ nm). $(n_{tol}/n_s)^2$ corrects for the difference in scattering volume of the solution and the toluene standard with refractive index n_{tol}.

In dilute solutions when interactions are weak, the weight-average molar mass (M_w), the z-average radius of gyration ($R_{gz} = \langle R_g^2\rangle^{0.5}$), and the second virial coefficient (A_2) can be derived using the so-called Zimm approximation:

$$\frac{KC}{I_r} = \frac{1}{M_w}\left(1 + \frac{(qR_{gz})^2}{3}\right)(1 + 2M_wA_2C) \qquad qR_{gz} < 1 \tag{3}$$

The intensity autocorrelation function measured with DLS ($g_2(t) = \langle I(0)\, I(t)\rangle/\langle I\rangle$) is related to the normalized electric field correlation function, $g_1(t)$, by the Siegert relation.[19] $g_1(t)$ was analyzed in terms of a distribution of relaxation times:

$$g_1(t) = \int A(\tau)\exp(-t/\tau)\, d\tau \tag{4}$$

using the Laplace inversion routine REPES.[20] This method does not assume a specific form for $A(\tau)$ but has a tendency to represent broad monomodal distributions by multiple peaks. Therefore, we also used the so-called generalized exponential (GEX) distribution: $A(\log\tau) = k\tau^p \exp[-(\tau/\tau^*)^s]$. The GEX distribution contains two parameters (p, s) to describe the shape of a wide range of single peaked distributions such as the Schultz−Zimm and the Pearson distribution. τ^* is the characteristic relaxation time, and k is a normalization constant.

If the relaxation of the concentration fluctuations is due to cooperative diffusion, the cooperative diffusion coefficient (D_c) may be calculated from the average relaxation rate $\langle\Gamma\rangle = \langle 1/\tau\rangle$ as $D_c = \langle\Gamma\rangle/q^2$.[19] In dilute solutions when interactions are weak, the z-average self-diffusion coefficient (D_z) and the dynamic second virial coefficient (k_D) can be derived utilizing

$$D_c = D_z(1 + k_DC) \qquad qR_{gz} < 1 \tag{5}$$

D_z is related to the z-average hydrodynamic radius ($R_{hz} = \langle 1/R_h\rangle_z^{-1}$) via the so-called Stokes−Einstein relation:

$$D_z = kT/6\pi\eta R_{hz} \tag{6}$$

with k Boltzmann's constant and η the solvent viscosity.

Results and Discussion

Native Ovalbumin. We have used SLS and DLS to characterize aqueous solutions of ovalbumin at pH 7 either with just 3 mM NaN_3 to protect against bacterial degradation or with in addition 0.1 M NaCl to screen electrostatic interactions. The scattering intensity of all solutions was independent of the scattering wave vector within the experimental error, because the radius of the particles is small compared to q^{-1} in the range covered by light scattering. In Figure 1 the concentration dependence of KC/I_r is compared for the two ionic strengths. Extrapolation to $C = 0$ gives the weight-averaged molar mass of ovalbumin, which is the same at both ionic strengths: $M_w = 4.6 \times 10^4$ g/mol. The experimental value of M_w is close to that of ovalbumin monomers.

The concentration dependence of KC/I_r is much stronger at the lower ionic strength due to electrostatic interactions that are partially screened by the presence of 0.1 M NaCl. From the initial linear concentration dependence we estimated the second virial coefficient: $A_2 = 2.5 \times 10^{-6}$ L mol g^{-2} at 3 mM NaN_3 and $A_2 = 2.2 \times 10^{-7}$ L mol g^{-2} at 0.1 M NaCl. The linear increase of KC/I_r extends to about 50 g/L at the higher ionic strength, after which the contribution of ternary interactions becomes significant. At lower ionic strength the concentration dependence weakens above approximately 10 g/L. The reason is that counterions of the proteins contribute to the ionic strength so that electrostatic interaction is progressively screened with increasing protein concentration.

The intensity autocorrelation functions of ovalbumin solutions were characterized by two distinct relaxation

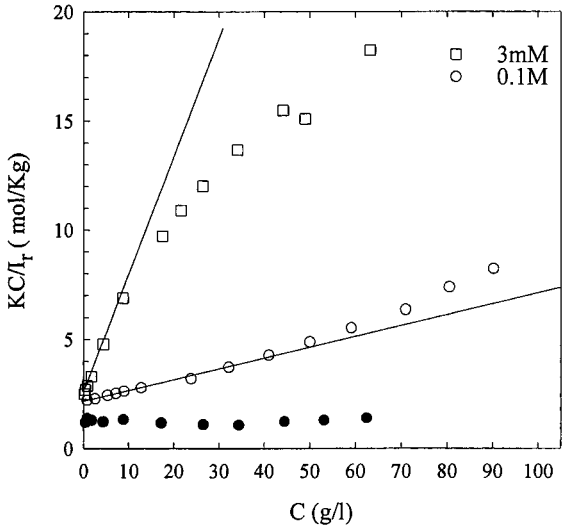

Figure 1. Concentration dependence of KC/I_r of native ovalbumin at pH 7 and two ionic strengths (open symbols). The filled symbols represent the results for ovalbumin solutions at $\mu = 3$ mM heated at 78 °C for 20 h.

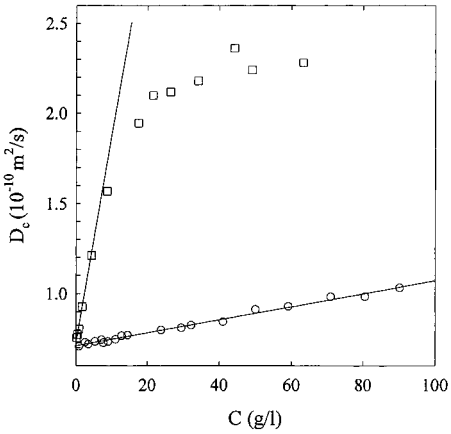

Figure 2. Concentration dependence the cooperative diffusion coefficient of native ovalbumin at pH 7 and two ionic strengths. The symbols are as in Figure 1.

modes. The average relaxation rate of both modes was q^2-dependent. The slower mode decreased in amplitude after filtration and could be completely removed at lower concentrations, without significant reduction of the protein concentration. We believe that the fast mode is due to cooperative diffusion of ovalbumin monomers and that the slow mode is due to self-diffusion of a very small weight fraction of large protein aggregates. At higher concentrations a slow mode with relatively weak amplitude remained even after careful filtration. Therefore, we have corrected I_r for the scattering by these large aggregates.

In Figure 2 the concentration dependence of D_c at the two ionic strengths is compared. Extrapolation to $C = 0$ gives $D_z = 7.1 \times 10^{-11}$ m^2/s at both ionic strengths. The hydrodynamic radius calculated utilizing eq 6 is 2.9 nm, in agreement with the value reported by Nemoto et al.[9] The concentration dependence of D_c is again much stronger at lower ionic strength due to electrostatic interactions. From the initial concentration dependence we estimated the dynamic second virial coefficient: $k_D = 0.1$ L/g at 3 mM NaN_3 and $k_D = 5.1 \times 10^{-3}$ L/g at 0.1 M NaCl. The concentration dependence of D_c is determined both by thermodynamic interactions and friction. The former cause D_c to increase with increasing concentration whereas the latter causes it to decrease. The results obtained here for ovalbumin resemble those obtained for β-lactoglobulin, which was studied in detail at the same pH and ionic strengths.[21]

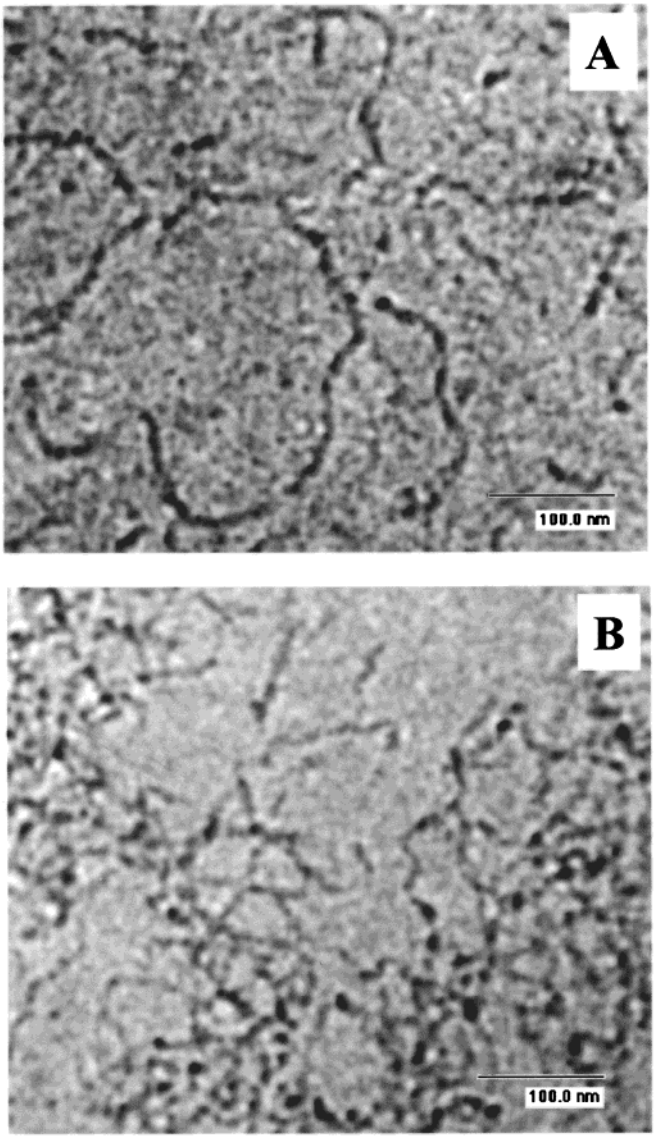

Figure 3. Cryo-TEM micrographs of ovalbumin aggregates formed after heat treatment in 3 mM NaN_3 (a) or in 0.1 M NaCl (b). The samples were heated for 22 h at 78 °C with $C =$ 54 g/L in 3 mM NaN_3 and $C = 5.4$ g/L at 0.1 M NaCl. Micrographs were obtained for diluted samples ($C = 0.5$ g/L in 3 mM NaN_3 and $C = 1$ g/L at 0.1 M NaCl).

Dilute Ovalbumin Aggregates. We have characterized ovalbumin aggregates formed after heating solutions with different protein concentrations at 78 °C for 20 h. The aggregates were highly diluted so that the effect of interactions and multiple scattering could be neglected and were studied at 20 °C using SEC, SLS, DLS, and cryo-tem. Ovalbumin solutions at 3 mM NaN_3 remain transparent when heated, whereas at 0.1 M NaCl they become turbid. At the lower ionic strength the solutions gel if $C > 60$ g/L and an insoluble gel fraction is visible after dilution, whereas at 0.1 M NaCl the solutions gel if $C > 12$ g/L.

Figure 3 shows cryo-TEM micrographs of large ovalbumin aggregates formed after heat treatment in 3 mM NaN_3 or in 0.1 M NaCl. The samples were heated for 22 h at 78 °C at concentrations (54 g/L at 3 mM NaN_3

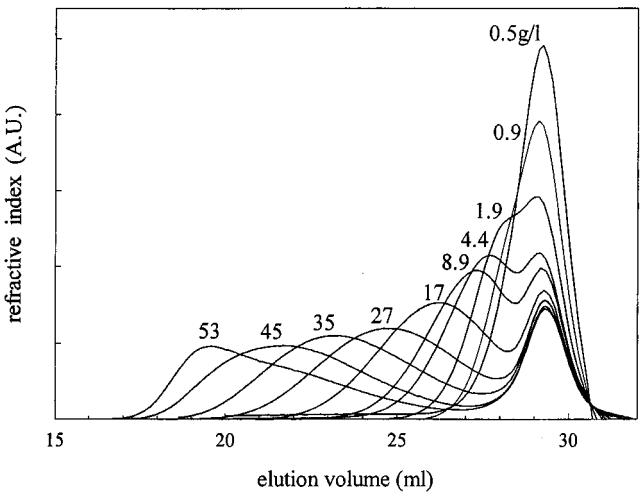

Figure 4. Chromatographs of ovalbumin solutions at pH 7 and $\mu = 3$ mM heated at 78 °C for 20 h.

and 5.4 g/L at 0.1 M NaCl) that were chosen such that aggregates are formed with R_{gz} about 300 nm at both ionic strengths. At low ionic strength long flexible aggregates are formed with very few branch points. The diameter of the aggregates is 6 ± 1 nm, in agreement with the results at low ionic strength obtained by Koseki et al.[11] using transmission electron microscopy. This results suggest a simple linear aggregation of monomeric ovalbumin and not the aggregation of dimers suggested by Nemoto et al.[9] on the basis of light scattering results. In the presence of 0.1 M NaCl more densely branched clusters are observed, but the elementary structure of clusters is again monomeric ovalbumin. It appears that the aggregation of ovalbumin at pH 7 is essentially the same at different ionic strengths but that branching is inhibited by electrostatic repulsion.

Figure 4 shows chromatograms of heated ovalbumin solutions with a range of protein concentrations at 3 mM NaN_3. At the lowest concentrations one observes a broadening of the size distribution toward smaller elution volumes, i.e., larger sizes, compared to native ovalbumin, but for $C > 2$ g/L two distributions can be distinguished. The narrow peak at an elution volume of about 29 mL corresponds to unaggregated protein while the second peak broadens and shifts to smaller elution volumes with increasing concentration. Similar results are obtained in the presence of 0.1 M NaCl, except that the increase of the average aggregate size occurs at lower protein concentrations. The fraction of unaggregated protein can be deduced from the surface area of the corresponding peak in the chromatograms if it is well resolved. This fraction is about 27% independent of the protein concentration for $C > 5$ g/L. At lower concentrations the fraction of unaggregated ovalbumin is difficult to establish and increases with decreasing concentration. At 0.1 M NaCl we also found a fraction of about 27% unaggregated ovalbumin at all concentrations investigated.

It has been reported that ovalbumin may transform into a thermally more stable conformation[22] and that the fraction of this so-called S-ovalbumin depends on the history of the batch.[23] For one solution (9.5 g/L, 0.1 M) we determined the fraction of unaggregated ovalbumin as a function of heating time at 78 °C. We found that this fraction decreases at first rapidly to an apparent plateau at about 30% after which it continues to decrease very slowly. This result together with the

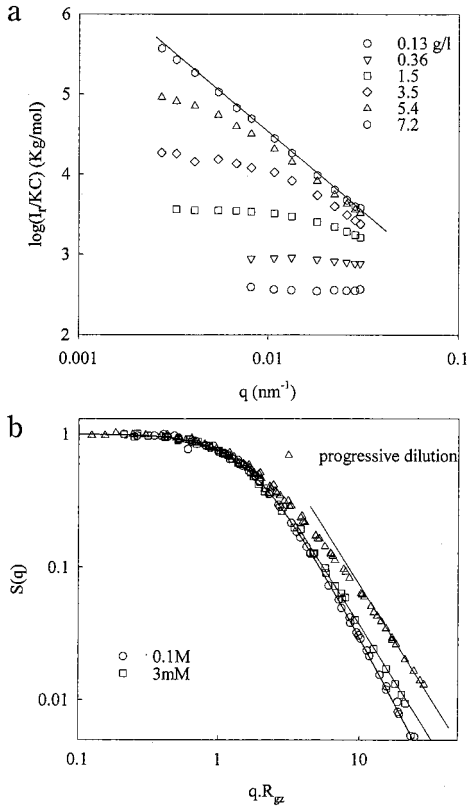

Figure 5. (a) Double-logarithmic representation of the q dependence of I_r/KC for ovalbumin solutions at pH 7 and $\mu =$ 0.1 M heated at 78 °C for 20 h. The line has slope −2.0. (b) Structure factor of highly diluted ovalbumin aggregates formed at pH 7 and two ionic strengths. The triangles represent the structure factor of interpenetrated ovalbumin aggregates obtained by progressive dilution of a solution containing very large ovalbumin aggregates (>1 μm) formed at low ionic strength. The solid line through the circles represents $S(qR_{gz}) = (1 + (qR_{gz})^2/3)^{-1}$. The straight lines through the squares and triangles have slope −1.7.

SEC results indicates that the batch used in these experiments contains about 27% thermally stable ovalbumin.

For each highly diluted sample we measured the q dependence of the scattering intensity and the correlation function. At 0.1 M NaCl the contribution of unaggregated ovalbumin to I_r is negligible for all systems investigated whereas without NaCl this is the case for $C > 5$ g/L. Figure 5a shows the q dependence of I_r/KC for heated ovalbumin solutions at 0.1 M NaCl. With increasing concentration larger aggregates are formed which leads to an increase of I_r/KC at $q \rightarrow 0$, i.e., M_w for highly diluted samples, and a stronger q dependence. Just below the concentration where a gel is formed I_r has a power law dependence on q, which means that we probe the internal, self-similar structure of the aggregates. The aggregates are characterized by a fractal dimension d_f that relates the molar mass to the radius of gyration: $M \propto R_g^{d_f}$. The fractal dimension can also be determined from the q dependence of I_r: $I_r \propto q^{-d_f}$ for $qR_g \gg 1$.[24] The solid line in Figure 1 has slope −2.0, from which we deduce $d_f = 2.0$.

Often the structure factor of aggregates formed by a random aggregation process is a unique function of qR_{gz}. This means that if $(I_r/KC)/M_w$, i.e., $S(q)$, is plotted as a function of qR_{gz}, all data collapse on to a single master curve. Such master curves have been reported earlier for aggregates formed after heat denaturation for two

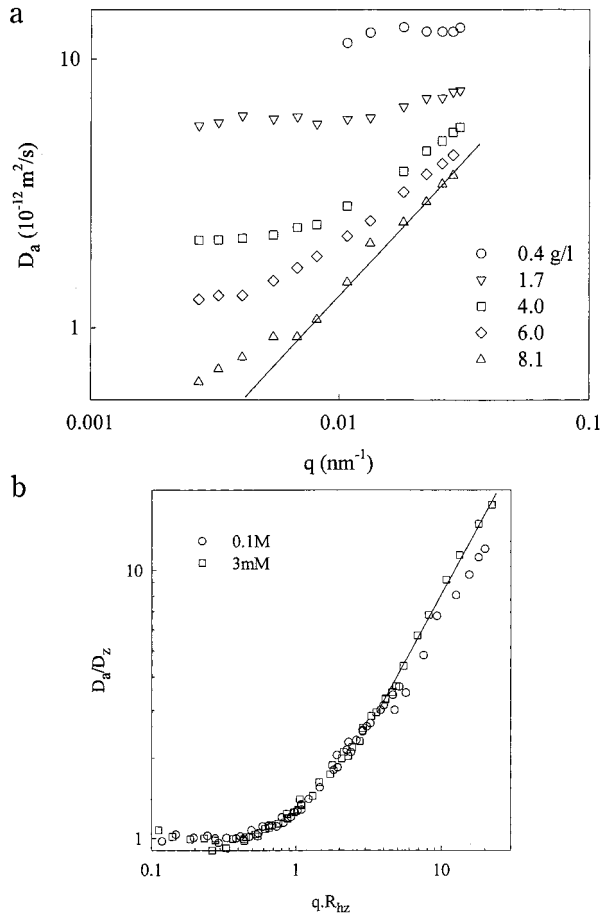

Figure 6. (a) Double-logarithmic representation of the q dependence of the apparent diffusion coefficient for ovalbumin solutions at pH 7 and $\mu = 0.1$ M heated at 78 °C for 20 h. The solid line has slope one. (b) Normalized representation of the data shown in (a) plus the results obtained at $\mu = 3$ mM. The solid line has slope one.

other globular proteins: β-lactoglobulin[12] and BSA.[14] For ovalbumin we also obtain master curves, at both ionic strengths (see Figure 5b), which shows that the structure factor of the aggregates is a unique function of qR_{gz}. However, the functional form of $S(qR_{gz})$ depends on the ionic strength. At 0.1 M NaCl the structure factor is well-described by the following equation: $S(qR_{gz}) = (1 + (qR_{gz})^2/3)^{-1}$. The same function described $S(qR_{gz})$ for β-lactoglobulin aggregates formed at the same conditions.[25] The structure factor of aggregates formed at low ionic strength deviates from this function at large values of qR_{gz}. Even though the structure factor depends on the ionic strength at which the aggregates are formed, it is the same whether the aggregates are diluted in 3 mM NaN_3 or in 0.1 M NaCl. This implies that dilution in salt only decreases electrostatic repulsion and does not change the structure factor of aggregates.

The correlograms could in all cases be well described by a monomodal q^2-dependent relaxation time distribution, and the apparent diffusion coefficient was calculated as $D_a = \langle\Gamma\rangle/q^2$. The q dependence of D_a is shown in Figure 6a for aggregates formed at different ovalbumin concentrations at 0.1 M NaN_3. At low concentrations $qR_{gz} < 1$ over the whole q range so that D_a is independent of q and equal to D_z. At higher concentrations larger aggregates are formed, and one observes the influence of internal dynamics. Master curves can be formed at both ionic strengths by plotting D_a/D_z as a function of qR_{hz} (see Figure 6b). Notice that since $D_z \propto 1/R_{hz}$, we only use one independent parameter in the construction of the master curves. For $qR_{hz} > 5$ we find $D_a \propto q$, which is expected for flexible particles.[26] At $\mu = 3$ mM the limiting linear dependence of D_{app} on q is reached at lower values of qR_{gz} than at $\mu = 0.1$ M, which could mean that the aggregates formed at higher ionic strength are slightly less flexible.

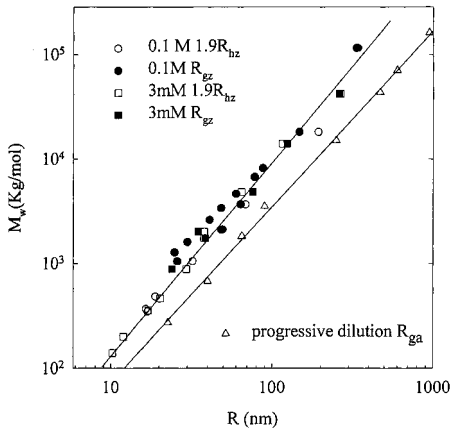

Figure 7. Dependence of R_{gz} and R_{hz} on M_w for ovalbumin aggregates formed at pH 7 and two ionic strengths. The line through the data has slope −1.8. The values of $1.9R_{hz}$ are shown to demonstrate that $R_{gz} \approx 1.9R_{hz}$. The triangles show the dependence of M_a on R_{ga} for progressive dilutions of a solution containing very large ovalbumin aggregates (>1 μm) formed at low ionic strength. The line through the data has slope −1.65.

The construction of the master curves allows one to determine M_w, R_{gz}, and R_{hz} even if eqs 3 and 5 are no longer valid. For all systems we observed that $R_{gz} \approx 1.9R_{hz}$ within the experimental error. Notice that since $R_{gz} = \langle R_g^2\rangle^{0.5}$ and $R_{hz} = \langle 1/R_h\rangle_z^{-1}$, polydispersity increases the ratio R_{gz}/R_{hz}. Figure 7 shows that M_w has a power law dependence on R_{gz} and R_{hz}, which is within the experimental error the same for the two ionic strengths. Koseki et al.[11] reported values of M_w and R_{gz} over a narrower range for ovalbumin aggregates formed in 20 mM salt at pH 7. Their results are close to the present results after correction for the slightly different refractive index increment used to calculate M_w. As mentioned above, the fractal dimension of the aggregates can be obtained either by utilizing $S(qR_{gz}) \propto q^{-d_f}$ at $qR_{gz} \gg 1$ or by utilizing $M_w \propto R_{gz}{}^{d_f}$. The first method gives $d_f = 2.0$ at $\mu = 0.1$ M and $d_f = 1.7$ at $\mu = 3$ mM. The dependence of the molar mass on the radius of the aggregates gives a single intermediate value ($d_f = 1.8$) but is nevertheless consistent in view of the considerable scatter of the data.

The size of the aggregates increases with increasing ovalbumine concentration and diverges at a given concentration C_{gel} (see Figure 8). In 3 mM NaN_3 the size of the aggregates increases monotonically from a value close to that of native ovalbumine, whereas in 0.1 M NaCl the size of the aggregates is already several times larger than that of native ovalbumin even at the lowest concentration at which reliable measurements could be done.

It should be remembered, however, that the data were obtained at a given heating time and temperature. After this heat treatment all active ovalbumin has aggregated, but only a small fraction of inactive ovalbumin has aggregated. To calculate the molar mass of the aggregates, one needs to use the concentration and scattering intensity of just the aggregates in eq 3 and

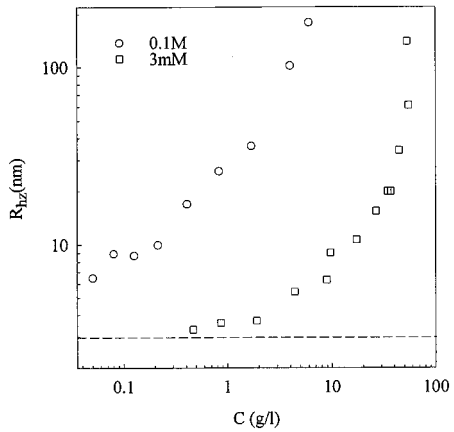

Figure 8. Concentration dependence of the hydrodynamic radius of ovalbumin aggregates formed after heating at 78 °C for 20 h at pH 7 and two ionic strengths. The dashed line indicates the hydrodynamic radius of native ovalbumin.

not the total protein concentration. As mentioned above, the contribution of unaggregated proteins to the scattered light is in most cases negligible. However, the aggregate concentration is about 27% smaller than the total protein concentration except at very low concentrations where it is even smaller. This means that M_w of just the aggregates is about 27% larger than that of the total system. The values of R_{gz} and R_{hz} are not influenced by the presence of unaggregated proteins, because the concentration does not enter in the calculation of these parameters.

Microscopy showed that at low ionic strength essentially semiflexible linear aggregates are formed. The fractal dimension of linear chains in good solvents is about 1.7[26] at length scales larger than the persistence length, which is consistent with the present experimental results. Linear aggregates were also observed for β-lactoglobulin at pH 2, but not at pH 7.[27] At pH 7 and low ionic strength heat denatured β-lactoglobulin forms small well-defined so-called primary aggregates for $C < 40$ g/L. Above this concentration the aggregate size increases with increasing concentration and β-lactoglobulin solutions gel for C larger than about 75 g/L. Cryo-TEM shows that the small primary aggregates have an elongated shape. If electrostatic interactions are screened by the presence of 0.1 M salt, the primary aggregates randomly associate to form larger self-similar aggregates and eventually a gel for $C > 7$ g/L. Similar association also occurs without added salt at higher protein concentrations because counterions progressively screen electrostatic interactions. A study of the structure of the larger β-lactoglobulin aggregates formed at low ionic strength is currently being pursued.

The results described so far were obtained using batch I. A number of experiments were repeated using batch II. The results were the same except that the fraction of heat stable ovalbumin is somewhat smaller in this batch (about 20%).

Undiluted Ovalbumin Solutions. We have studied undiluted heated ovalbumin solutions at 3 mM NaN_3 using SLS and DLS. At 0.1 M NaCl heated ovalbumin solutions become turbid, and special equipment is needed in order to correct for multiple scattering. With increasing concentration the heated systems are increasingly viscous, and for $C > 60$ g/L they no longer flow when tilted. The q dependence of the scattering intensity of the heated solutions is negligible, which

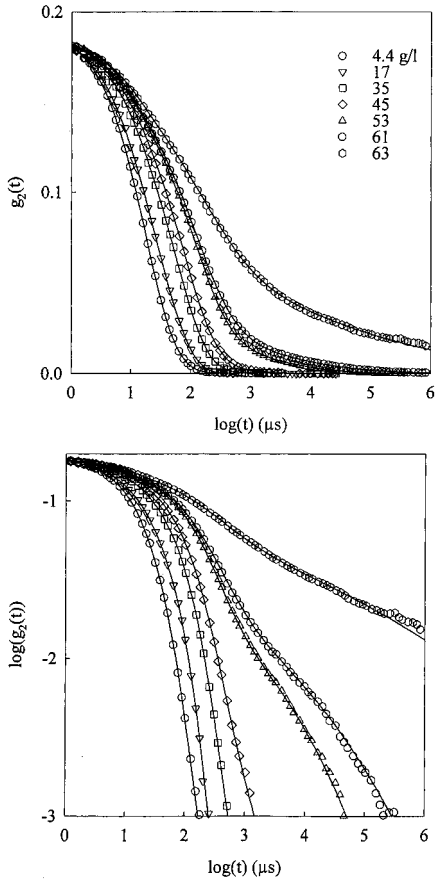

Figure 9. Semi (top) and double (bottom) logarithmic representation of the normalized autocorrelation functions of ovalbumin solutions at different concentrations that were heated at 78 °C for 20 h and subsequently cooled to 20 °C (pH 7 and $\mu = 3$ mM). The solid lines represent nonlinear least-squares fits described in the text.

shows that the correlation length of the concentration fluctuations is less than 15 nm. KC/I_r is remarkably independent of the protein concentration (see Figure 1), implying that at these heating conditions the variation in aggregate size compensates for the variation in the interactions.

On the other hand, the correlograms obtained with DLS have a clear concentration dependence (see Figure 9). The left panel of Figure 10 shows the corresponding relaxation time distributions. Below 10 g/L we observe a single relaxation process whereas above this concentration we can distinguish two modes. At even higher concentrations we observe a third slow relaxation mode, which is better seen in the double-logarithmic representation of the correlation functions. The terminal relaxation time of this process increases strongly over a small concentration range and is outside the window of observation for $C > 61$ g/L. The correlation functions could be very well described by a sum of two log-normal relaxation time distributions and one generalized exponential distribution (see solid lines in Figure 9). Details of this fit procedure can be found in ref 28.

The relaxation times of the first two modes are q^{-2}-dependent, and the diffusion coefficients are plotted as a function of the concentration in Figure 11. For comparison, we also show D_c of the solutions before heating. The relative amplitude of the fastest relaxation mode (1) is about 10% independent of the concentration, and its diffusion coefficient, D_1, is close to D_c. We believe that mode 1 is caused by the cooperative diffusion of

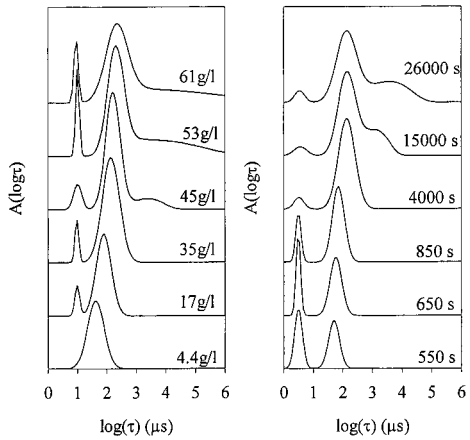

Figure 10. Relaxation time distributions corresponding to the correlation functions shown in Figure 9 (left panel) and Figure 13a (right panel). The results shown in the left panel were obtained for ovalbumin solutions at different concentrations that were heated at 78 °C for 20 h and subsequently cooled to 20 °C (pH 7 and $\mu = 3$ mM). The results shown in the right panel were obtained in situ for an ovalbumin solution at $C =$ 70 g/L at different heating times at 74 °C.

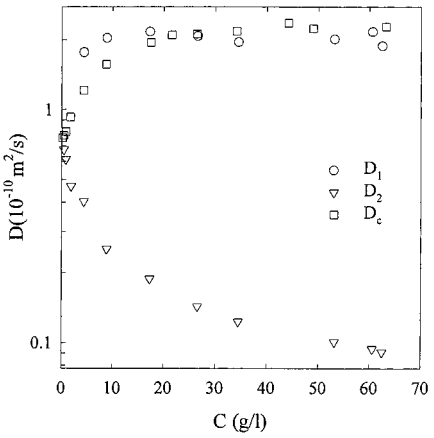

Figure 11. Cooperative diffusion coefficient of unaggregated ovalbumin (D_1) and aggregated ovalbumin (D_2) as a function of the concentration at which the solutions were heated at 78 °C for 20 h (pH 7 and 3 mM). For comparison, the concentration dependence of the cooperative diffusion coefficient of native ovalbumin (D_c) is shown at the same pH and ionic strength.

the fraction of unaggregated ovalbumin and that the slower diffusional mode (2) is caused by the cooperative diffusion of aggregated ovalbumin. We have seen with SEC (see Figure 4) that at very low concentrations only small aggregates are formed so that their diffusion process cannot be well distinguished from that of native ovalbumin. With increasing concentration larger aggregates are formed resulting in a decrease of D_2 and a better separation of the two relaxation modes. At higher protein concentrations interaction between the protein aggregates compensates for the growth of the aggregates, resulting in a weaker concentration dependence. The average relaxation time of the third mode has a very strong q dependence (about $\tau \propto q^{-4}$) and increases rapidly with the protein concentration close to C_{gel}. The relative amplitude of the third mode is about 15% at 45 g/L and 40% at 53 and 61 g/L.

We have measured the scattering intensity during the heating process at 77.5 °C for three protein concentrations (see Figure 12): a relatively low concentration (17 g/L) where rather small aggregates are formed after

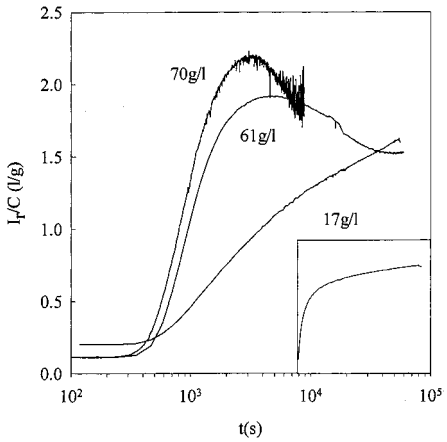

Figure 12. Dependence on heating time at 77.5 °C of I_r/C for ovalbumin solutions at three concentrations (pH 7 and 3 mM). The inset shows the result for $C = 17$ g/L with a linear time axis.

20 h ($R_{gz} = 20$ nm), a concentration (61 g/L) where very large aggregates are formed ($R_{gz} > 1$ μm), and a concentration (70 g/L) where the system gels. After placing the solutions in the apparatus it takes about 500 s to reach the set heating temperature. Thus, at short times we measure the scattering intensity of unaggregated ovalbumine. As discussed above, I_r/C for native ovalbumine is larger at 17 g/L than at the two higher concentrations caused by strong repulsive electrostatic interactions. When the temperature of the solutions increases, the intensity increases because the proteins aggregate. At the lowest concentration I_r increases first rapidly after which the increase slows down. At long times the increase is approximately logarithmic and appears to stagnate in a lin−lin representation (see inset of Figure 12). The initial rise of I_r is caused by aggregation of the active ovalbumin fraction whereas the logarithmic growth at longer times is probably caused by slow aggregation of thermally more stable ovalbumin.

At higher protein concentrations I_r rises rapidly to a maximum, after which it slowly decreases. The initial increase of I_r is caused by the increase of the number and size of the linear aggregates. Once the size and concentration of the linear aggregates is such that they start to overlap I_r reaches a maximum. Above this overlap concentration (C^*), I_r decreases weakly with increasing concentration but is independent of further growth of the aggregates as is expected for semidilute solutions of linear chains.[26] Notice that I_r/C after 20 h heating is approximately independent of the concentration. For the highest concentration I_r shows fluctuations around the average value that increase in amplitude with heating time, the origin of which will be discussed below. A similar observation has been reported for β-lactoglobulin.[29]

We measured the correlation functions at different times during the aggregation process for $C = 70$ g/L at 74 and at 77 °C. The evolution of I_r/C is the similar at the two temperatures, but the process is about 4 times slower at 74 °C than at 77 °C. Results obtained at 74 °C are plotted on a semilogarithmic scale in Figure 13a, while results obtained at 77 °C are plotted on a double-logarithmic scale in Figure 13b. The right panel of Figure 10 shows the relaxation time distributions corresponding to the correlation functions in Figure 13a. Even at the earliest stages of the aggregation process we observed two distinct relaxation modes. The faster

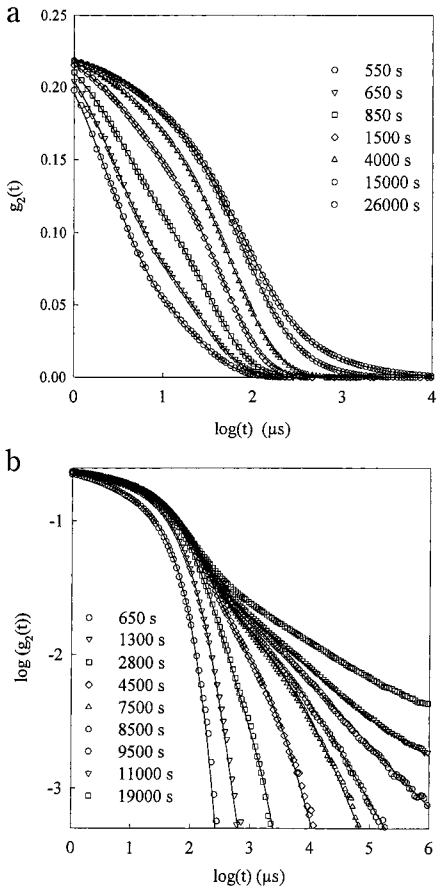

Figure 13. (a) Semilogarithmic representation of autocorrelation functions of ovalbumin solutions at $C = 70$ g/L at different heating times at 74 °C (pH 7 and 3 mM). The solid lines represent nonlinear least-squares fits. (b) Double-logarithmic representation of autocorrelation functions of ovalbumin solutions at $C = 70$ g/L at different heating times at 77 °C (pH 7 and 3 mM). The solid lines represent nonlinear least-squares fits.

mode is due to the diffusion of unaggregated proteins, and the slower mode is due the diffusion of aggregates. The relative amplitude of the fast mode decreases rapidly and stabilizes at about 6% at both temperatures. Chromatographs obtained from SEC at different heating times also showed that even when the large majority of the proteins has not yet aggregated, the aggregate peak is well separated. This feature, which was reported earlier by Koseki et al.,[11] has also been observed for β-lactoglobulin.[12]

At longer heating times when I_r approaches the maximum, a third very slow mode appears, which is more clearly seen in a double-logarithmic representation (see Figure 13b). With increasing heating time the terminal relaxation time of mode 3 increases and becomes longer than the time over which I_r is averaged (about 10 s). This is the reason I_r fluctuates strongly around the average value in Figure 12 at long heating times. The relative amplitude of mode 3 increases with heating time and is about 35% close to the gel point. Preliminary measurements of the evolution of the shear modulus showed that the appearance of very slow intensity fluctuations is correlated with a sharp rise of the storage shear modulus.

Figure 14 shows the dependence on heating time of the average relaxation time of the three modes. The average relaxation time of mode 1 (τ_1) is independent of heating time, and the corresponding diffusion coefficient is close to that of unheated ovalbumin. The average relaxation time of mode 2 (τ_2) increases first with heating time and then stabilizes or even decreases very weakly. The third mode can be first detected after τ_2 has reached its maximum. Its average relaxation time (τ_3) increases rapidly and diverges at the heating time where the large fluctuations of I_r appear. Varying the temperature only varies the rate at which the system develops. At lower ovalbumin concentrations the evolution of the system is similar, but the aggregation process stagnates at an earlier stage.

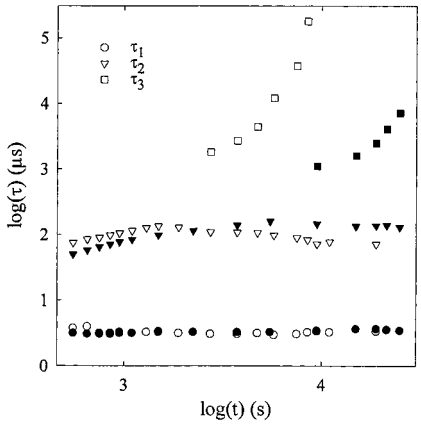

Figure 14. Average relaxation times of the three relaxation modes of ovalbumin solution at $C = 70$ g/L as a function of heating time at 74 °C (filled symbols) and 77 °C (open symbols).

Results similar to those shown in Figures 12 and 13 have been reported earlier for other gel-forming systems. Especially, many features observed here show a remarkable resemblance with those observed during the copolymerization of methyl methacrylate (MMA) with a small fraction of ethylene glycol dimethacrylate (EGDMA) in solution.[28,30] This copolymerization process leads to the formation of linear polymethacrylate (PMMA). The EGDMA units incorporated in the linear PMMA chains form cross-links as the system approaches the overlap concentration. Similarly, we interpret the present results at low ionic strength as follows. Initially, the fraction of active ovalbumin forms mainly linear aggregates. This aggregation process stagnates when all active ovalbumin has aggregated. The larger is the concentration of active ovalbumin the larger are the linear aggregates. Above a given ovalbumin concentration the linear aggregates reach the overlap concentration and have a small probability to form junctions. The very slow relaxation process may be interpreted in terms of self-diffusion of branched aggregates. A very strong q dependence of the relaxation time points to anomalous diffusion; i.e., the effective friction coefficient increases if the aggregates diffuse over a larger distance. Above C_{gel} the branched aggregates percolate and form a gel.

Progressive Dilution of an Ovalbumin Solution Close to the Gel Point. An ovalbumin solution with $C = 60$ g/L at 3 mM NaN3 was heated for 22 h at 78 °C. After cooling to 20 °C the solution was progressively diluted with 0.1 M NaCl, and SLS and DLS measurements were done at each dilution. As mentioned above, the q dependence of I_r is negligible for undiluted solutions. After dilution, I_r increases and the q dependence becomes stronger. After dilution by more than a factor 300, I_r has a power law q dependence over the whole accessible q range. Curves at different dilutions are similar to those shown in Figure 5a. For each

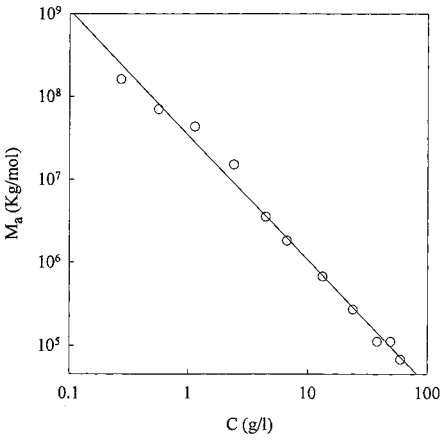

Figure 15. Dependence of the apparent molar mass on the concentration for progressive dilutions of a solution containing very large ovalbumin aggregates (>1 μm) formed at $\mu = 3$ mM and pH 7.

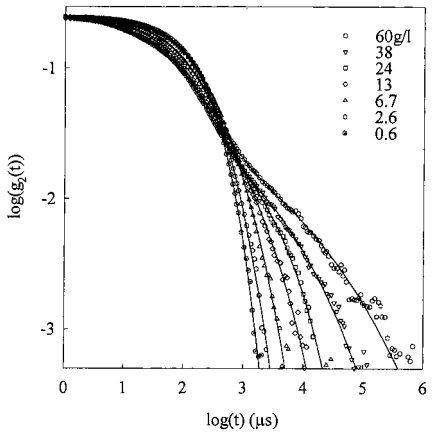

Figure 16. Double-logarithmic representation of autocorrelation functions of different dilutions of an ovalbumin solution at $C = 60$ g/L that was heated at 78 °C for 20 h (pH 7 and 3 mM). The solid lines represent nonlinear least-squares fits.

dilution we determined an apparent molar mass (M_a) and radius of gyration (R_{ga}) using $KC/I_r = (1 + (qR_{ga})^2/3)/M_a$. M_a is proportional to the osmotic compressibility of the system, and R_{ga} is proportional to the correlation length of the concentration fluctuations. Again, a master curve can be formed by plotting $(I_r/KC)/M_a$ as a function of qR_{ga}. The master curve which represents the structure factor of the progressively diluted systems is compared in Figure 5b with the structure factor of the highly diluted aggregates formed at different concentrations.

Naturally, the limiting power law q dependence at $qR_{ga} \gg 1$ is the same for both structure factors and depends on the fractal dimension of the aggregates. The crossover to this limiting power law behavior is different, however, because in the case of progressive dilution one measures the cutoff of the fractal structure at the correlation length of the system, whereas in the case of highly diluted aggregates one measures the cutoff of the fractal structure at the radius of gyration.

In Figure 7 we compare the dependence of M_a on R_{ga} for progressively diluted solutions with that of M_w on R_{gz} of highly diluted aggregates. Again, we observe a power law dependence: $M_a \propto R_{gz}^{-1.65}$. Within the experimental error the power law exponent is the same as for highly diluted samples, but the prefactor is smaller in the case of progressively diluted solutions. The smaller prefactor is consistent with the more gradual transition of $S(q)$ to its limiting power law q dependence at large qR_{gz}. The concentration dependence of M_a is shown in Figure 15. For semidilute solutions of flexible polymers in good solvents $\pi \propto C^{2.3}$ is expected theoretically[26] and observed experimentally.[31] Utilizing eq 1, one expects for such systems $M_a \propto C^{-1.3}$, which may be compared to $M_a \propto C^{-1.5}$ obtained here (see solid line in Figure 15).

As discussed above for undiluted samples close to the gel point the correlograms are characterized by three relaxational modes: (1) the diffusion of inactive ovalbumin, (2) the cooperative diffusion of the aggregates, and (3) a broad slow mode often observed in gelling systems which could be due to self-diffusion of branched aggregates. Figure 16 shows the correlograms at different dilutions. One clearly observes the contribution of the three relaxation modes at the higher concentrations. The relaxation time of mode 1 is not modified much by dilution, but the relative amplitude decreases when the system is diluted and becomes negligible for $C < 10$ g/L. The relaxation time of mode 3 decreases rapidly with increasing dilution, while that of mode 2 increases weakly. For $C < 2$ g/L the two modes have merged, and the correlation functions are well described by a monomodal relaxation time distribution.

The static and dynamic light scattering results may be understood if we assume that the system consists of mainly linear interpenetrated aggregates with a small fraction of branched clusters. When the system is diluted, the correlation length increases, which leads to decrease of the cooperative diffusion coefficient. Dilution also leads to a decrease of the viscosity and thus to faster diffusion of the branched clusters. Again, there is a resemblance with cross-linked PMMA.[30] Progressive dilution of cross-linked PMMA close to the gel point also leads to a rapid decrease of the relaxation time of mode 3 until it merges with mode 2. However, the concentration dependence of the scattering intensity is much stronger for cross-linked PMMA ($M_a \propto C^{-3}$) and is consistent with theoretical predictions for the dilution of percolating clusters. The results reported here for ovalbumin are closer to that expected for the dilution of linear chains. Another difference is that the maximum of the size distribution of cross-linked PMMA remains situated at the position of linear PMMA formed in the absence of EGDMA and simply broadens with increasing reaction time. This result is again consistent with the prediction of percolating clusters. For ovalbumin the maximum shifts with increasing reaction time. We conclude that branching of the linear ovalbumin aggregates formed at low ionic strength is not very important unless the system is very close to the gel point. A few measurements of progressive dilution of β-lactoglobulin aggregates at pH 2 showed qualitatively the same effects as for ovalbumin.[32]

Conclusion

Heated ovalbumin at pH 7 forms linear aggregates of monomeric ovalbumin, with very little branching at low ionic strength, but with strong branching at 0.1 M NaCl. The aggregates are semiflexible and have a self-similar structure characterized by a fractal dimension of 1.7 at low ionic strength and 2.0 at 0.1 M NaCl.

At low ionic strength heated ovalbumin solutions remain transparent and can be studied with light scattering techniques. The scattering intensity increases

with heating time until the linear aggregates start to overlap, after which the intensity decreases. The correlation length of the solutions at low ionic strength remains small due electrostatic interactions, which explains why they remain transparent. The degree of branching increases when the aggregates overlap and leads to gel formation for concentrations above 60 g/L. Progressive dilution shows that the system close to the gel point is similar to a semidilute solution of flexible polymers.

The concentration fluctuations fully relax by cooperative diffusion for concentrations below the gel point. At concentrations approaching the gel point an additional slow relaxation process is observed possibly caused by self-diffusion of aggregates and restructuration. The terminal relaxation time becomes very long when the gel is formed, which leads to slow fluctuations of the scattering intensity.

Acknowledgment. We thank Martien Cohen Stuart for stimulating discussions.

References and Notes

(1) Clark, A. H. In *Functional Properties in Food Macromolecules*; Mitchell, J. R., Ed.; Elsevier Applied Science: London, 1998; pp 77−142.
(2) Creamer, L. K.; Jimenez-Flores, R.; Richardon, T. *Trends Biotechnol.* **1988**, *6*, 163.
(3) Mine, Y. Recent advances in the understanding of egg white protein functionality. *Trends Food Sci. Technol.* **1995**, *6*, 225.
(4) Croguennec, T.; Nau, F.; Pezennec, S.; Brule, G. *J. Agric. Food Chem.* **2000**, *48*, 4883.
(5) Nisbet, A. D.; Saundry, R. H.; Moir, A. J. G.; Fothergill, L. A.; Fothergill, J. E. *Eur. J. Biochem.* **1981**, *115*, 335.
(6) Perlmann, G. E. *J. Den. Physiol.* **1952**, *35*, 711.
(7) Linderstrøm-Lang, K.; Ottesen, M. *C. R. Trav. Lab. Carlsberg, Ser. Chim.* **1949**, *26*, 403.
(8) Hatta, H.; Kitabatake, N.; Doi, E. *Agric. Biol. Chem.* **1986**, *50*, 2083.
(9) Nemoto, N.; Koike, A.; Osaki, K.; Koseki, T.; Doi, E. *Biopolymers* **1993**, *33*, 551.
(10) Mine, Y. *J. Agric. Food Chem.* **1996**, *44*, 2086.
(11) Koseki, T.; Kitabatake, N.; Doi, E. *Food Hydrocolloids* **1989**, *3*, 123.
(12) Gimel, J. C.; Durand, D.; Nicolai, T. *Macromolecules* **1994**, *27*, 583.
(13) Le Bon, C.; Nicolai, T.; Kuil, M. E.; Hollander, J. G. *J. Phys. Chem. B* **1999**, *103*, 10294.
(14) Hagiwara, T.; Kumagai, H.; Nakamura, K. *Biosci., Biotechnol., Biochem.* **1996**, *60*, 1757.
(15) Barbano, D. M.; Clark, J. L.; Dunham, C. E.; Flemming, J. R. *J. Assoc. Off. Anal. Chem.* **1990**, *73*, 849.
(16) Verhoef, J. C.; Barendrecht, E. *Anal. Chim. Acta* **1977**, *94*, 395.
(17) Brown, W., Ed. *Light Scattering. Principles and Developments*; Clarendon Press: Oxford, 1996.
(18) Higgins, J. S.; Benoit, K. C. *Polymers and Neutron Scattering*; Clarendon Press: Oxford, 1994.
(19) Berne, B.; Pecora, R. *Dynamic Light Scattering*; Wiley: New York, 1976.
(20) Stepanek, P. In *Dynamic Light Scattering*; Brown, W., Ed.; Oxford University Press: Oxford, 1993.
(21) Le Bon, C.; Nicolai, T.; Durand, D. *Int. J. Food Sci. Technol.* **1999**, *34* (5/6), 451.
(22) Smith, M. B.; Back, J. F. *Nature (London)* **1962**, *193*, 878.
(23) Schäfer, A.; Drewes, W.; Schwägele, F. *Nahrung* **1999**, *43*, 86.
(24) Nicolai, T.; Durand, D.; Gimel, J. C. In *Light Scattering. Principles and Developments;* Brown, W.; Ed.; Clarendon Press: Oxford, 1996; Chapter 6.
(25) Nicolai, T.; Urban, C.; Schurtenberger, P. *J. Colloid Interface Sci.* **2001**, *240*, 419.
(26) de Gennes, P. G. *Scaling Concepts in Polymer Physics;* Cornell University Press: London, 1979.
(27) Durand, D.; Gimel, J. C.; Nicolai, T. *Physica A* **2002**, *304*, 253.
(28) Lesturgeon, V.; Nicolai, T.; Durand, D. *Eur. Phys. J. B* **1999**, *9*, 71.
(29) Takata, S.; Norisuye, T.; Tanaka, N.; Shibayama, M. *Macromolecules* **2000**, *33*, 5470.
(30) Lesturgeon, V.; Nicolai, T.; Durand, D. *Eur. Phys. J. B* **1999**, *9*, 83.
(31) Noda, I.; Kato, N.; Kitano, T.; Ngasawa, M. *Macromolecules* **1981**, *14*, 668.
(32) Aymard, P.; Nicolai, T.; Durand, D.; Clark, A. *Macromolecules* **1999**, *32*, 2542.

MA0120198